Applied Geochemistry 101 (2019) 19–30

Contents lists available at ScienceDirect

Applied Geochemistry

journal homepage: www.elsevier.com/locate/apgeochem

A Helmholtz free energy equation of state for the vapor-liquid equilibrium and *PVTx* properties of the H_2S–H_2O mixture and its application to the H_2S–H_2O–NaCl system

Chuanrong Peng[a], Shide Mao[a,*], Jiawen Hu[b], Limei He[a]

[a] School of Earth Sciences and Resources, China University of Geosciences, Beijing, 100083, China
[b] College of Resources, Hebei GEO University, Shijiazhuang, 050031, China

ARTICLE INFO

Editorial handling by Dr D A. Kulik

Keywords:
H_2S–H_2O
H_2S–H_2O–NaCl
Equation of state
PVTx
Phase equilibria

ABSTRACT

An equation of state (EOS) explicit in Helmholtz free energy has been developed to calculate the vapor-liquid equilibrium (VLE) and pressure-volume-temperature-composition (*PVTx*) properties of the H_2S–H_2O fluid mixture. This EOS, where five mixing parameters are used, is based on the highly accurate EOSs of pure H_2S and H_2O fluids, and contains a simple departure function. Compared to reliable experimental data available, the average absolute deviations of H_2S solubility in liquid phase, water content in vapor phase, and liquid density of the H_2S–H_2O system are 3.88%, 5.03% and 0.20%, respectively. The EOS of the H_2S–H_2O fluid mixture, together with the Pitzer activity coefficient of H_2S in aqueous NaCl solution from previous study, can be used to predict the H_2S solubility in aqueous NaCl solution with an average absolute deviation of 7.52%. The water content of vapor phase in the H_2S–H_2O–NaCl system can be reproduced with the fluid EOS of H_2S–H_2O system by a fugacity-activity method within experimental uncertainties. The fluid EOS of H_2S–H_2O system, combined with the Helmholtz free energy EOS of H_2O–NaCl fluid mixture, can predict the *PVTx* properties of the H_2S–H_2O–NaCl mixture without using additional mixing parameters. The developed EOS can be safely used under the conditions of CO_2 capture and sequestration (273–473 K, 0–400 bar and 0–6 mol kg^{-1}), beyond which the EOS also has some extrapolated ability. The computer codes are in the supplemental data and can be downloaded from Applied Geochemistry or obtained from the corresponding author.

1. Introduction

H_2S is one of important acid gases, which has been frequently reported as one of the components of natural gases (Li et al., 2005; Worden et al., 1995) and fluid inclusions in the host minerals (Cai et al., 2015; Giuliani et al., 2003). Sulfur-based compounds (H_2S and SO_x) have always been found with CO_2 (the major greenhouse gas) in flue gases generated from power plants and other large-scale industrial processes. To reduce the emission of greenhouse gases, deep saline formations approximated by the NaCl–H_2O system have been regarded as the best storage option for their high potential capacity (Emami-Meybodi et al., 2015; Firoozabadi and Myint, 2010; Jafari Raad and Hassanzadeh, 2017), and the co-injection of both CO_2 and H_2S into deep saline formations will reduce the costs of CO_2 capture and sequestration (CCS) (Gunter et al., 2000; Knauss et al., 2005). Therefore, knowledge of the vapor-liquid equilibrium (VLE) and pressure-volume-temperature-composition (*PVTx*) properties of the H_2S–H_2O and H_2S–H_2O–NaCl systems under conditions of CCS (generally below 473 K and 300 bar) is an indispensable step to assess the safety and cost benefit before the co-sequestration of CO_2 and H_2S in deep saline formations.

Since the last century, many experimental data have been reported for the VLE properties of the H_2S–H_2O and H_2S–H_2O–NaCl systems, but the *PVTx* data are very scarce for the H_2S–H_2O system and no experimental volumetric data have been found for the H_2S–H_2O–NaCl system (Table 1). The VLE data are still scattered, and most of them cover a limited pressure-temperature-composition (*P-T-x*) space, inconvenient to use. Therefore, theorists devoted extensive efforts to modeling the VLE and/or *PVTx* properties of the H_2S–H_2O and H_2S–H_2O–NaCl systems so as to interpolate among experimental data points or extrapolate beyond the data range (Table 2).

Dubessy et al. (2005) presented an asymmetric model to calculate the VLE properties of the H_2S–H_2O–NaCl system up to 523 K and 6 molality of NaCl, which is based on a cubic equation of state (EOS) for

* Corresponding author.
E-mail address: maoshide@163.com (S. Mao).

https://doi.org/10.1016/j.apgeochem.2018.12.021
Received 17 May 2018; Received in revised form 10 December 2018; Accepted 14 December 2018
Available online 20 December 2018
0883-2927/

Table 1
Experimental VLE and *PVTx* datum sets for the H_2S–H_2O and H_2S–H_2O–NaCl systems.

References	*T* (K)	*P* (bar)	m_{NaCl} (mol·kg^{-1})	N_d (Types)
H_2S–H_2O				
Hnědkovský et al. (1996)	298.15–705.53	10–350	0	30 (*PVTx*)
Zezin et al. (2011)	523.15–673.15	80.5–239.0	0	44 (*PVTx*)
McLauchlan (1903)	298.2	0.09–0.14*	0	5 (*PTx*)
Winkler (1906)	273.15–363.15	1.013	0	14 (*PTx*)
Pollitzer (1909)	298.2	1.013	0	1 (*PTx*)
Kendall and Andrews (1921)	298.15	1.013	0	1(*PTx*)
Dede and Becker (1926)	293.2	1	0	1 (*PTx*)
Wright and Maass (1932a)	278.15–333.15	0.8–4.7	0	35 (*PTx*)
Wright and Maass (1932b)	278.15–333.15	0.36–4.94	0	104 (*PTxy*)
Kiss et al. (1937)	273.2–298.2	1.013	0	3 (*PTx*)
Kapustinsky (1941)	298.2	1.013*	0	1 (*PTx*)
Selleck et al. (1952)	310.92–444.26	6.89–206.84	0	110 (*PTxy*)
Pohl (1961)	303.1–316.1	17.24	0	30 (*PTxy*)
Kozintseva (1965)	433.15–603.15	0.85–2.10*	0	28 (*PTxy*)
Harkness and Kelman (1967)	303.15	1.013	0	1 (*PTx*)
Burgess and Germann (1969)	303.15–443.15	17.2–23.4	0	78 (*PTxy*)
Clarke and Glew (1971)	273.15–323.14	0.4–1	0	72 (*PTxy*)
Gerrard (1972)	273.15–298.15	1	0	4 (*PTx*)
Lee and Mather (1977)	283.2–453.2	1.5–66.7	0	340 (*PTx*,*PTy*)
Douabul and Riley (1979)	275.25–302.97	1.013	0	7 (*PTx*)
Drummond (1981)	304.05–627.85	7.1–195.0	0	121 (*PTx*)
Gillespie and Wilson (1982)	311–589	3–207	0	92 (*PTxy*)
Byeseda et al. (1985)	297.1	1.016*	0	1 (*PTx*)
Barrett et al. (1988)	296.65–367.65	1.013	0	39 (*PTx*)
Suleimenov and Krupp (1994)	293.95–594.15	2.22–138.61	0	98 (*PTxy*)
Kuranov et al. (1996)	313.15–313.18	4.7–24.9	0	9 (*PTx*)
Chapoy et al. (2005)	298.16–338.34	4.97–39.62	0	46 (*PTx*,*PTy*)
Koschel et al. (2007)	323.1–393.1	17.2–320.7	0	12 (*PTx*)
Savary et al. (2012)	393.15–423.15	17–325	0	6 (*PTx*)
H_2S–H_2O–NaCl				
Drummond (1981)	299.05–673.15	6.47–300.91	1–6.15	353 (*PTx*)
Barrett et al. (1988)	299.15–369.65	1.013	1–5	230 (*PTx*)
Suleimenov and Krupp (1994)	428.35–593.95	11.96–138.42	0.24–2.54	46 (*PTxy*)
Xia et al. (2000)	313.13–393.19	2.5–97	4, 6	71 (*PTx*)
Savary et al. (2012)	393.15–423.15	17–325	2	5 (*PTx*)
Koschel et al. (2013)	323.1–393.1	17.6–311.7	1, 3, 5	20 (*PTx*)

Notes: *T* is temperature (K); *P* is pressure (bar), and superscript "*" represents the partial pressure of H_2S; m_{NaCl} is the molality of NaCl; N_d is the number of data points, and *PVTx*, *PTx*, *PTy* and *PTxy* in brackets denote the volumetric data, and the phase equilibrium data of liquid, vapor and vapor-liquid phases.

Table 2
Thermodynamic models for the VLE and/or *PVTx* properties of the H_2S–H_2O and H_2S–H_2O–NaCl systems since 2000.

References	*T* (K)	*P* (bar)	m_{NaCl} (mol·kg^{-1})
Dubessy et al. (2005)	273–523	0–150	0–6
Duan et al. (2007)	273–500	0–200	0–6
Perfetti et al. (2008)	333–453	0–120	0
Li and Firoozabadi (2009)	310–589	1–210	0
Tsivintzelis et al. (2010)	310.9–444.3	1–210	0
dos Ramos and McCabe (2010)	200–603	0–600	0
Ji and Zhu (2010, 2012)	273–673	0–300	0–6
Kunz and Wagner (2012)	303–589	3–207	0
Zirrahi et al. (2012)	283–393	1–204	0–6
Bacon et al. (2014)	298–477	0–200	0–2
Li et al. (2015)	273–523	1–200	0–6
Springer et al. (2015)	273–573	0–345	0 – saturation
Akinfiev et al. (2016)	283–573	1–400	0–6

Notes: *T* is temperature (K); *P* is pressure (bar); m_{NaCl} is the molality of NaCl.

the descriptions of vapor phase and the Henry's and Raoult's laws for the descriptions of liquid phase, but this model is valid to 150 bar. Duan et al. (2007) developed a model based on a virial EOS of H_2S and the Pitzer electrolyte theory to predict H_2S solubility in pure water and aqueous NaCl solution (273–500 K, 0–200 bar and 0–6 molality of NaCl in water). However, the model cannot calculate the water content of vapor phase. Perfetti et al. (2008) proposed a cubic plus association (CPA) EOS together with the mean spherical approximation theory to model the phase equilibria of the H_2S–H_2O system, but the valid *T-P* range is limited to 333–453 K and 0–120 bar. Li and Firoozabadi (2009) developed a CPA EOS to calculate the VLE properties of the H_2S–H_2O system with a valid *T-P* range of 310–589 K, and 1–210 bar, which can well predict the water content of the H_2S-rich vapor or liquid phase. Tsivintzelis et al. (2010) proposed a CPA EOS to model the phase equilibria for acid gases including the H_2S–H_2O system with a valid *T-P* range of 310.9–444.3 K, and 1–210 bar. dos Ramos and McCabe (2010) developed a statistical associating fluid theory (SAFT) EOS with the generalized mean spherical approximation (GSMA) to model the VLE properties of the H_2S–H_2O system, covering a wide *T-P* range of 200–603 K and 0–600 bar. Ji and Zhu (2010, 2012) established a SAFT EOS to predict the VLE and *PVTx* properties of the H_2S–H_2O and H_2S–H_2O–NaCl systems with a valid *T-P-*m_{NaCl} (molality of NaCl in water) range of 273–673 K, 0–300 bar and 0–6 mol kg^{-1}. Kunz and Wagner (2012) developed a Helmholtz free energy EOS (GERG-2008) for natural gases and other mixtures including the H_2S–H_2O system. However, the H_2S–H_2O system was treated as an ideal mixture, so this EOS shows large pressure deviations at VLE. Zirrahi et al. (2012) presented a model coupled with the Henry's law approach for the phase equilibrium properties of the H_2S–H_2O–NaCl system, but the highest valid temperature is limited to 393 K. Bacon et al. (2014) developed a phase-equilibrium model for the H_2S–H_2O–NaCl system by a cubic EOS and two sets of different parameters for the vapor and liquid phases, whose form is similar to that of Soreide and Whitson (1992) (SW model). However, the valid salinity of the model is limited to 2 mol kg^{-1}. Based on the modification of the binary interaction parameters for aqueous phase in the SW model, Li et al. (2015) developed a cubic EOS for the phase equilibria of the H_2S–H_2O–NaCl system, but

its valid pressure range is only 0–200 bar. Springer et al. (2015) established a thermodynamic model for the phase and chemical equilibria of the H_2S–H_2O–NaCl system on the basis of EOSs for the standard-state properties of individual species, covering a valid T-P-m_{NaCl} range of 273–573 K, 0–345 bar and NaCl concentration from zero to saturation. Akinfiev et al. (2016) proposed a thermodynamic model for the H_2S–H_2O–NaCl system based on the Henry's law and the Pitzer interaction model, which is valid in the T-P-m_{NaCl} range of 273–573 K, 0–400 bar and 0–6 mol kg^{-1}. However, the partial pressure of water in the model is approximated as the saturation pressure of pure water, so it cannot be used to accurately predict the water content of vapor phase.

In this work, firstly, an accurate Helmholtz free energy EOS was developed to calculate the VLE and *PVTx* properties of the H_2S–H_2O fluid mixture. Secondly, the EOS of the H_2S–H_2O mixture, together with the Pitzer activity coefficient of H_2S developed by Duan et al. (2007), was applied to predict H_2S solubility in aqueous NaCl solution. Thirdly, the EOS of the H_2S–H_2O mixture combined with the osmotic coefficient of aqueous NaCl solution from Pitzer et al. (1984) was applied to predict the water content of vapor phase of the H_2S–H_2O–NaCl system. Finally, the Helmholtz free energy EOSs of binary H_2S–H_2O and H_2O–NaCl mixtures were combined to predict the *PVTx* properties of the ternary H_2S–H_2O–NaCl mixture using the approach of Mao et al. (2015b).

2. Review of experimental VLE and *PVTx* data of the H_2S–H_2O and H_2S–H_2O–NaCl mixtures

The experimental data for the *PVTx* and VLE properties of the H_2S–H_2O and H_2S–H_2O–NaCl fluid mixtures since last century are summarized in Table 1. Only two data sets have been found for the *PVTx* properties of the H_2S–H_2O mixture up to 705 K and 350 bar. Hnědkovský et al. (1996) and Zezin et al. (2011) measured the molar volumes of liquid and vapor phases of the H_2S–H_2O system, respectively. The data of Hnědkovský et al. (1996) are internally consistent with high accuracy, which cover a wide T-P range from 298 to 705 K and from 10 to 350 bar. However, the volumetric data of Zezin et al. (2011) are in the near-critical region and yield large deviations in the parameterization of EOS, so they are not used in this work.

The VLE properties of the H_2S–H_2O mixture have been measured over a relatively wide T-P range. The pressure-temperature-liquid composition-vapor composition (*PTxy*) data of the H_2S–H_2O mixture (273–589 K and 0.4–207 bar) were reported by Wright and Maass (1932b), Selleck et al. (1952), Pohl (1961), Kozintseva (1965), Burgess and Germann (1969), Clarke and Glew (1971), Gillespie and Wilson (1982) and Suleimenov and Krupp (1994), which were directly used in the fitting except for some extrapolated data of Selleck et al. (1952). The data of H_2S solubility in pure water reported by McLauchlan (1903), Winkler (1906), Pollitzer (1909), Kendall and Andrews (1921), Dede and Becker (1926), Wright and Maass (1932a), Kiss et al. (1937), Kapustinsky (1941), Harkness and Kelman (1967), Clarke and Glew (1971), Gerrard (1972), Douabul and Riley (1979), Byeseda et al. (1985) and Barrett et al. (1988) are of temperatures up to 368 K with pressures below 5 bar. Most of these data are consistent with each other within experimental uncertainties except for some data of Barrett et al. (1988) with temperatures above 354 K. Kuranov et al. (1996), Lee and Mather (1977), and Chapoy et al. (2005) reported the H_2S solubility in water at moderate pressures up to 67 bar, and these data are highly accurate. Lee and Mather (1977) and Chapoy et al. (2005) also reported the water content of vapor phase from 0.5 to 34 bar. However, some data of Lee and Mather (1977) at 393 K are discrete and unreliable. The data of H_2S solubility in water reported by Drummond (1981), Koschel et al. (2007) and Savary et al. (2012) are of high pressures up to 325 bar and most of these data are reliable. The single *PTx* or *PTy* data of the H_2S–H_2O system above cannot be directly used in the fitting, but they can testify the validation of the EOS of the H_2S–H_2O mixture.

There are six data sets for the H_2S solubility in aqueous NaCl solution and one set for the water content of vapor phase of the H_2S–H_2O–NaCl mixture. The data of H_2S solubility in aqueous NaCl solution published by Drummond (1981) cover a wide T-P-m_{NaCl} range (299–673 K, 7–300 bar and 0–6 mol kg^{-1}). However, as mentioned by Akinfiev et al. (2016), these data exhibit large differences between the heating and cooling processes, and the average discrepancy between them is more than 10%. The data of Barrett et al. (1988) at 1 atm cover the temperature range of 299–369 K, but Barrett et al. (1988) themselves pointed out that some data of 368 K have large experimental errors up to 15%. Suleimenov and Krupp (1994) reported the *PTxy* data of the H_2S–H_2O–NaCl mixture with the T-P-m_{NaCl} range of 428–594 K, 12–138 bar and 0.2–2.5 mol kg^{-1}, and these data are reliable. The data of H_2S solubility in aqueous NaCl solution at VLE reported by Xia et al. (2000) are highly accurate. Most of the data of H_2S solubility in aqueous NaCl solution from Savary et al. (2012) and Koschel et al. (2013) are reliable, except for the two data of Savary et al. (2012) near 200 bar.

3. EOS of the H_2S–H_2O fluid mixture

The EOS of the H_2S–H_2O mixture is in terms of dimensionless Helmholtz free energy α defined as

$$\alpha = \frac{A}{RT} \tag{1}$$

where A is the molar Helmholtz free energy, R is the molar gas constant (8.314472 J mol^{-1} K^{-1}), and T is the temperature in K.

The dimensionless Helmholtz free energy α of mixture is separated into two parts:

$$\alpha = \alpha^0 + \alpha^r \tag{2}$$

where α^0 and α^r are the ideal-gas part and the residual part of Helmholtz free energy of mixture, respectively. The superscripts "0" and "r" denote the ideal-gas part and the residual part. The α^0 in Eq. (2) is defined as:

$$\alpha^0 = \sum_{i=1}^{N} x_i[\alpha_i^0(\rho, T) + \ln x_i] \tag{3}$$

where ρ is the density of mixture, x_i is the mole fraction of component i, N is the number of components in mixture, and α_i^0 is the ideal-gas part of dimensionless Helmholtz free energy of component i.

The α^r in Eq. (2) is defined as

$$\alpha^r = \sum_{i=1}^{N} x_i \alpha_i^r(\delta, \tau) + \alpha^E \tag{4}$$

where α_i^r is the residual part of dimensionless Helmholtz free energy of component i, α^E is the excess energy of mixture, and δ and τ are the reduced parameters of mixture:

$$\delta = \frac{\rho}{\rho_c}, \quad \tau = \frac{T_c}{T} \tag{5}$$

where ρ_c and T_c are the pseudo-critical density and temperature of mixture, whose forms are the same as those of Kunz and Wagner (2012):

$$\rho_c = \left[\sum_{i=1}^{N} x_i^2 \frac{1}{\rho_{c,i}} + \sum_{i=1}^{N-1}\sum_{j=i+1}^{N} 2x_i x_j \beta_{v,ij}\gamma_{v,ij}\frac{x_i + x_j}{\beta_{v,ij}^2 x_i + x_j}\frac{1}{8}\left(\frac{1}{\rho_{c,i}^{1/3}} + \frac{1}{\rho_{c,j}^{1/3}}\right)^3\right]^{-1} \tag{6}$$

$$T_c = \sum_{i=1}^{N} x_i^2 T_{c,i} + \sum_{i=1}^{N}\sum_{j=i+1}^{N} 2x_i x_j \beta_{T,ij}\gamma_{T,ij}\frac{x_i + x_j}{\beta_{T,ij}^2 x_i + x_j}(T_{c,i}T_{c,j})^{0.5} \tag{7}$$

where α_i^0 and $T_{c,i}$ are the critical density and critical temperature of component i, respectively, and $\beta_{v,ij}$, $\gamma_{v,ij}$, $\beta_{T,ij}$ and $\gamma_{T,ij}$ are the mixture-

Table 3
Coefficients and exponents in Eq. (8).

k	$n_{ij,k}$	$t_{ij,k}$	$d_{ij,k}$	$l_{ij,k}$
1	3.9440467×10^{-1}	0.880	1	0
2	-1.7634732	2.932	1	0
3	1.4620755×10^{-1}	2.433	3	0
4	8.752232×10^{-3}	1.330	0	1
5	2.0349398	4.416	2	1
6	-9.035025×10^{-2}	5.514	3	1
7	$-2.1638854 \times 10^{-1}$	5.203	1	2
8	3.9612170×10^{-2}	1.000	5	2

dependent binary parameters associated with components i (H_2S) and j (H_2O).

The α^E in Eq. (4) takes the following form:

$$\alpha^E = \sum_{i=1}^{N-1}\sum_{j=i+1}^{N} x_i x_j F_{ij}\left(\sum_{k=1}^{3} n_{ij,k}\delta^{d_{ij,k}}\tau^{t_{ij,k}} + \sum_{k=4}^{8} n_{ij,k}\delta^{d_{ij,k}}\tau^{t_{ij,k}}\exp(-\delta^{l_{ij,k}})\right) \tag{8}$$

where $n_{ij,k}$, $d_{ij,k}$, $t_{ij,k}$ and $l_{ij,k}$ are the parameters, whose values can be found from the EOS-CG model developed by Gernert and Span (2016) for the CO_2—H_2O mixture (Table 3), and F_{ij} is a mixture-dependent binary parameter of components i (H_2S) and j (H_2O).

In this work, the EOSs of pure H_2S (see Appendix A) and H_2O fluids are from Li (2017) and Wagner and Pruss (2002), respectively. The critical parameters and molar masses of H_2S and H_2O fluids are listed in Table 4.

The binary parameters ($\beta_{v,ij}$, $\gamma_{v,ij}$, $\beta_{T,ij}$, $\gamma_{T,ij}$ and F_{ij}) in above equations for the H_2S—H_2O mixture are determined by a regression to the experimental VLE data (Burgess and Germann, 1969; Clarke and Glew, 1971; Gillespie and Wilson, 1982; Kozintseva, 1965; Pohl, 1961; Selleck et al., 1952; Suleimenov and Krupp, 1994) and the *PVTx* data (Hnědkovský et al., 1996). In the fitting, the objective function is defined as the sum of relative deviations of molar volume and fugacity difference of each component in vapor and liquid phases. Regressed parameters are listed in Table 5.

The density or molar volume of the H_2S—H_2O mixture can be calculated from the following equation with the Newton iterative method:

$$P = \rho RT(1 + \delta\alpha_\delta^r) \tag{9}$$

where P is the pressure in bar, and α_δ^r is the derivative of α^r with respect to δ. The initial density of mixture can be set as the density of ideal gas below the saturation pressure or the saturated liquid density of pure H_2O above the saturation pressure. This EOS agrees well with the experimental density data of Hnědkovský et al. (1996) up to 706 K and 350 bar. The average and maximum deviations of liquid densities are 0.20% and 1.07%, respectively. However, this EOS deviates largely from the vapor density data of Zezin et al. (2011) from 523 to 673 K and from 80 to 239 bar, with the average deviation of about 20%. Therefore, the vapor density data are needed to testify the validity of this EOS in the future.

The fugacity and fugacity coefficient of components i in the H_2S—H_2O mixture can be calculated from the following equations (Mao et al., 2015a):

Table 4
Critical parameters and molar masses of pure fluids.

i	$T_{c,i}$ (K)	$\rho_{c,i}$ (g·cm^{-3})	M (g·mol^{-1})
H_2S	373.1	0.3473	34.08088
H_2O	647.096	0.322	18.015268

Notes: $T_{c,i}$ and $\rho_{c,i}$ are the critical temperature and pressure of pure fluid i, respectively; M is the molar mass of pure fluid i.

Table 5
Parameters of the H_2S—H_2O fluid mixture.

Mixture ij	$\beta_{T,ij}$	$\gamma_{T,ij}$	$\beta_{v,ij}$	$\gamma_{v,ij}$	F_{ij}
H_2S—H_2O	1.0186100	0.89528807	1.1049404	0.77512962	0.61788031

Note: Subscripts i and j refer to H_2S and H_2O, respectively.

$$f_i = x_i\rho RT\exp\left(\frac{\partial n\alpha^r}{\partial n_i}\right)_{T,V,nj} \tag{10}$$

$$\ln\varphi_i = \left(\frac{\partial n\alpha^r}{\partial n_i}\right)_{T,V,nj} - \ln(1 + \delta\alpha_\delta^r) \tag{11}$$

$$\left(\frac{\partial n\alpha^r}{\partial n_i}\right)_{T,V,nj} = \alpha^r + n\left(\frac{\partial\alpha^r}{\partial n_i}\right)_{T,V,nj} \tag{12}$$

$$n\left(\frac{\partial\alpha^r}{\partial n_i}\right)_{T,V,nj} = \delta\alpha_\delta^r\left[1 - \frac{1}{\rho_c}\left[\left(\frac{\partial\rho_c}{\partial x_i}\right)_{x_j} - \sum_{k=1}^{N} x_k\left(\frac{\partial\rho_c}{\partial x_k}\right)_{x_j}\right]\right]$$
$$+ \tau\alpha_\tau^r\frac{1}{T_c}\left[\left(\frac{\partial T_c}{\partial x_i}\right)_{x_j} - \sum_{k=1}^{N} x_k\left(\frac{\partial T_c}{\partial x_k}\right)_{x_j}\right] + \alpha_{x_i}^r - \sum_{k=1}^{N} x_k\alpha_{x_k}^r \tag{13}$$

where α_τ^r, $\alpha_{x_i}^r$ and $\alpha_{x_k}^r$ are the derivatives of α^r with respect to τ, x_i and x_k, respectively, f_i and φ_i are the fugacity and fugacity coefficient of component i, respectively, V is the total volume of mixture, n is the total amount of substance in mixture, n_i is the amount of substance of component i, and n_j stands for the set of the amounts of substance of all components other than i.

The vapor-liquid equilibrium compositions and densities of the H_2S—H_2O mixture at given temperature and pressure can be calculated by the iterative algorithm of Michelsen (1993). Tables 6 and 7 list the average deviations of this EOS from each data set for the H_2S solubility in water and the water content in the H_2S-rich vapor or liquid phase. Figs. 1 and 2 indicate that this EOS can accurately reproduce most of

Table 6
Calculated deviations of H_2S solubility in pure water.

References	T (K)	P (bar)	N_d	AAD (%)
McLauchlan (1903)	298.2	0.09–0.14*	5	1.14
Winkler (1906)	273.15–363.15	1.013	14	2.69
Pollitzer (1909)	298.2	1.013	1	2.67
Kendall and Andrews (1921)	298.15	1.013	1	3.79
Dede and Becker (1926)	293.2	1	1	3.39
Wright and Maass (1932a)	278.15–333.15	0.8–4.7	34	1.97
Wright and Maass (1932b)	278.15–333.15	0.36–4.94	52	2.08
Kiss et al. (1937)	273.2–298.2	1.013	3	1.95
Kapustinsky (1941)	298.2	1.013*	1	0.06
Selleck et al. (1952)	310.92–444.26	6.89–120.66	39	5.15
Pohl (1961)	303.1–316.1	17.24	15	2.38
Kozintseva (1965)	433.15–603.15	0.85–2.10*	14	5.15
Harkness and Kelman (1967)	303.15	1.013	1	4.07
Burgess and Germann (1969)	303.15–443.15	17.2–23.4	39	1.96
Clarke and Glew (1971)	273.15–323.14	0.4–1	36	1.83
Gerrard (1972)	273.15–298.15	1	4	3.19
Lee and Mather (1977)	283.2–453.2	1.5–66.7	325	3.40
Douabul and Riley (1979)	275.25–302.97	1.013	7	1.91
Gillespie and Wilson (1982)	311–589	3–207	42	5.37
Byeseda et al. (1985)	297.1	1.016*	1	0.93
Barrett et al. (1988)	296.65–354.15	1.013	32	4.77
Suleimenov and Krupp (1994)	293.95–594.15	2.22–138.61	48	8.93
Kuranov et al. (1996)	313.15–313.18	4.7–24.9	9	4.01
Chapoy et al. (2005)	298.16–338.34	4.97–39.62	31	6.25
Koschel et al. (2007)	323–393	17.2–320.7	12	4.97
Savary et al. (2012)	393.15–423.15	17–325	6	13.15

Notes: T is temperature (K); P is pressure (bar); Superscript "*" indicates that the corresponding P is the partial pressure of H_2S; AAD = $\Sigma|100(x_{cal}/x_{exp} - 1)|/N_d$, where x_{cal} and x_{exp} are the calculated and experimental H_2S solubilities in water, respectively, and N_d is the number of data points.

Table 7
Calculated deviations of water content in the H_2S – rich vapor or liquid phase.

References	T (K)	P (bar)	N_d	AAD (%)
Wright and Maass (1932b)	278.15–333.15	0.36–4.94	52	5.83
Selleck et al. (1952)	310.92–444.26	6.89–120.66	39	5.09
Pohl (1961)	303.1–316.1	17.24	15	3.05
Kozintseva (1965)	433.15–603.15	0.85–2.10*	14	0.90
Burgess and Germann (1969)	303.15–443.15	17.2–23.4	39	2.09
Clarke and Glew (1971)	273.15–323.15	0.4–1.0	36	1.60
Lee and Mather (1977)	363.2–423.2	14.9–34.0	15	18.89
Gillespie and Wilson (1982)	311–589	3–207	47	8.60
Suleimenov and Krupp (1994)	293.95–594.15	2.22–138.61	49	0.86
Chapoy et al. (2005)	298.16–318.21	0.5–2.8	15	11.31

Notes: T is temperature; P is pressure; AAD = $\Sigma|100(y_{cal}/y_{exp}-1)|/N_d$, where y_{cal} and y_{exp} are the calculated and experimental water content of the H_2S-rich vapor or liquid phase, respectively, and N_d is the number of data points.

experimental VLE data within or close to experimental uncertainties. The EOS of GERG-2008 is also added for comparisons in Figs. 1 and 2, from which it can be seen that our EOS is much better than the GERG-2008 EOS for the H_2S solubility in water and the two EOSs have similar accuracy for the water content in the H_2S-rich vapor or liquid phase.

4. Application to the H_2S–H_2O–NaCl system

4.1. Prediction of the H_2S solubility in aqueous NaCl solution

Duan et al. (2007) used a Pitzer formulation to account for the effect of salt on the activity coefficient of H_2S in water, whose parameters are obtained from experimental solubility data. The Pitzer formulation can be written as:

$$\ln \gamma^r_{H_2S} = 2(c_1 + c_2T + c_3/T + c_4P)m_{Na^+} + c_5 m_{Cl^-} m_{Na^+} \quad (14)$$

where T is the temperature in K and P is the pressure in bar. m_{Na^+} and m_{Cl^-} are the molality of Na^+ and Cl^-, respectively. The coefficients c_1, c_2, c_3, c_4 and c_5 are in Table B1 of Appendix B. $\gamma^r_{H_2S}$ is the relative activity coefficient of H_2S, which is related to the H_2S solubility in aqueous NaCl solution by the approximation: $\gamma^r_{H_2S} = m^o_{H_2S}/m_{H_2S}$, where $m^o_{H_2S}$ and m_{H_2S} are the H_2S molality in pure water and aqueous NaCl solution at the same temperature and pressure. Thus, m_{H_2S} can be obtained from the relationship:

$$m_{H_2S} = 55.508 x^o_{H_2S}/(1 - x^o_{H_2S})/\gamma^r_{H_2S} \quad (15)$$

where 55.508 is the molality of H_2O (in mol·kg^{-1}), and $x^o_{H_2S}$ are the mole fraction of H_2S in pure water which can be calculated from the EOS of H_2S–H_2O mixture developed above.

Table 8 shows the average absolute deviations of this model from each data set for the H_2S solubility in aqueous NaCl solution. Fig. 3 gives the comparisons between the results of our model and experimental data, which indicate that the model has good accuracy for the H_2S solubility in aqueous NaCl solution. Fig. 4 compares the calculated solubility curves of H_2S and CO_2 in aqueous NaCl solution against pressures at given temperatures (323.15 K, 393.15 K and 473.15 K) and NaCl concentrations (2, 4 and 6 mol kg^{-1}), where the CO_2 solubility is calculated by combining the EOS-CG model with the activity coefficient model of Mao et al. (2013). Apparently, the H_2S solubility is much larger than the CO_2 solubility at the same T-P-m_{NaCl} conditions. It suggests that if the greenhouse gas CO_2 is mixed with H_2S, the gas contents in the (NaCl + H_2O)-rich liquid phase will increase under the same conditions of CCS.

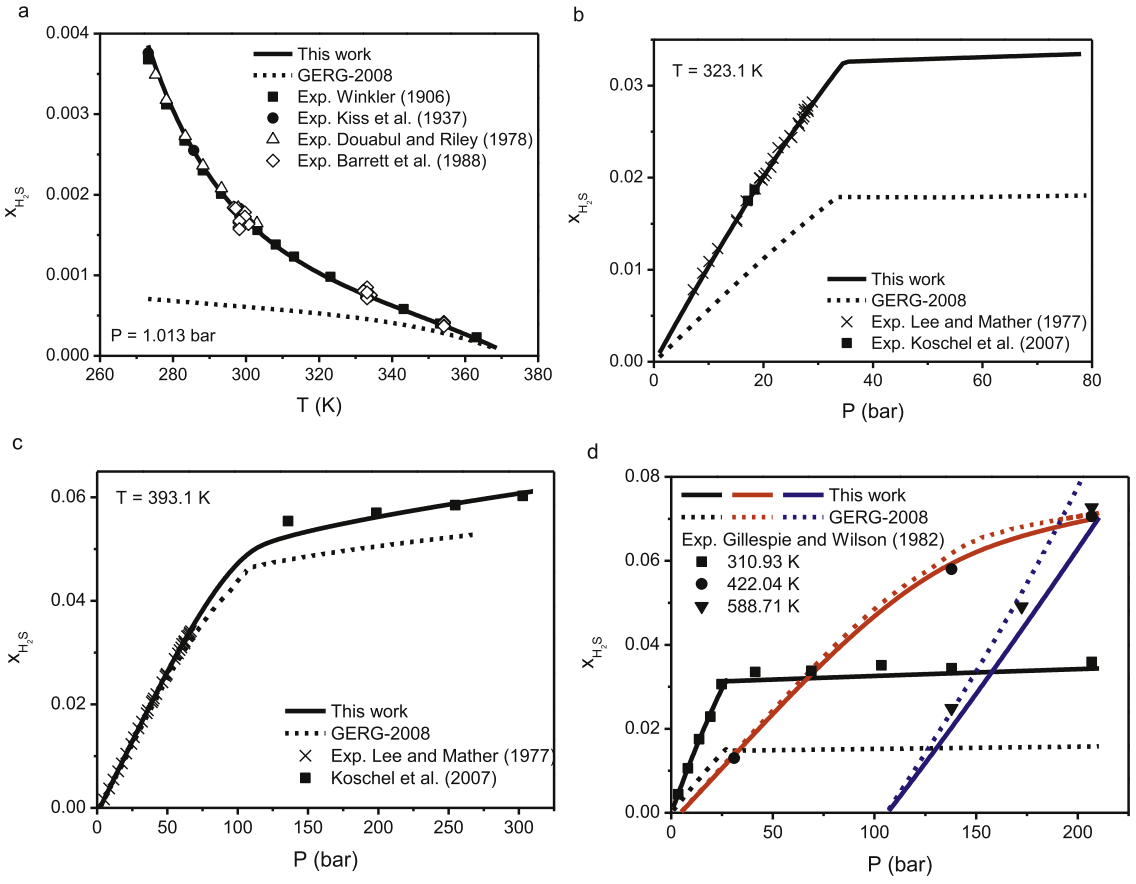

Fig. 1. H_2S solubility in water: T is temperature, P is pressure, and x_{H_2S} is the mole fraction of H_2S.

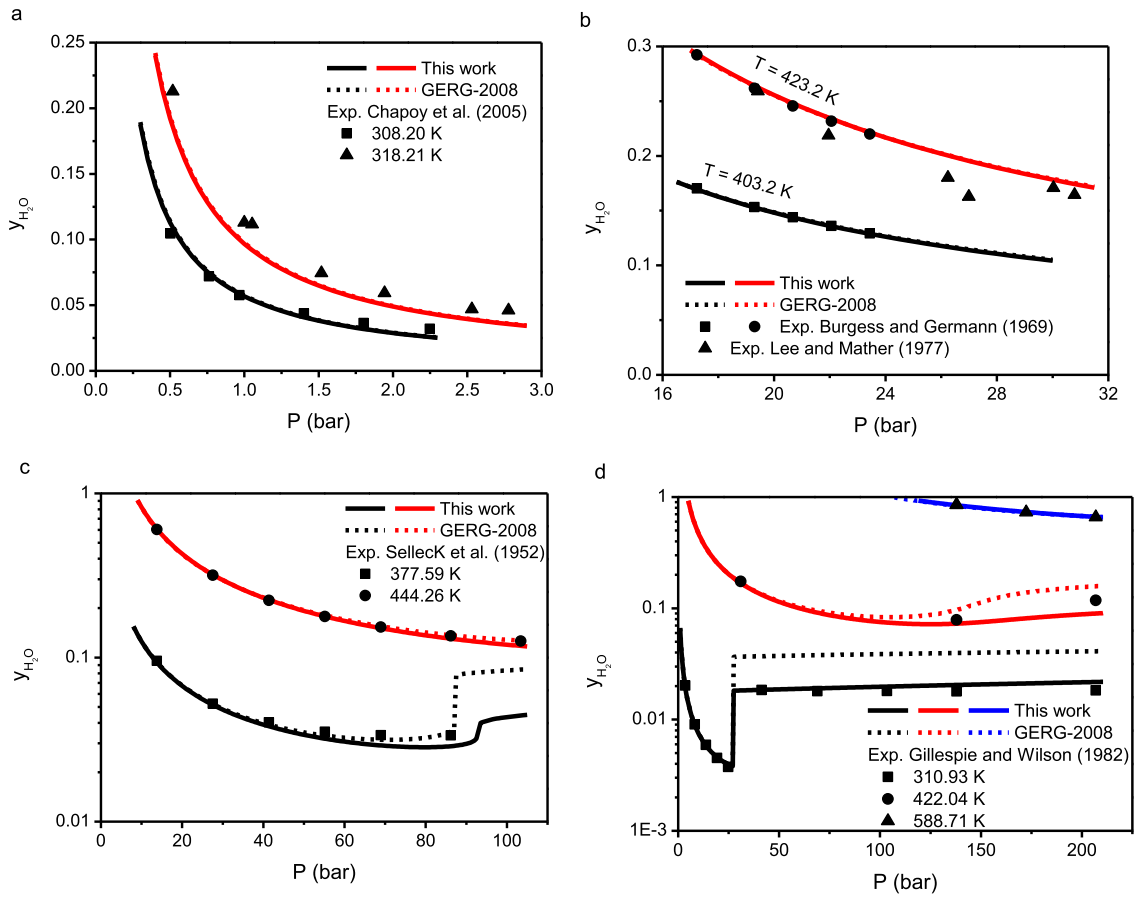

Fig. 2. Water content in the H_2S-rich vapor or liquid phase: T is temperature, P is pressure, and y_{H_2O} is the mole fraction of H_2O.

Table 8
Calculated deviations of H_2S solubility in aqueous NaCl solution.

References	T (K)	P (bar)	m_{NaCl} (mol·kg^{-1})	N_d	AAD (%)
Barrett et al. (1988)	296.15–358.15	1.013	1–5	151	8.44
Suleimenov and Krupp (1994)	428.35–593.95	11.96–138.42	0.24–2.54	23	6.08
Xia et al. (2000)	313.13–393.19	2.5–97	4, 6	57	4.30
Savary et al. (2012)	393.15	86–323	2	4	9.17
Koschel et al. (2013)	323.1–393.1	17.6–311.7	1, 3, 5	20	11.02

Notes: T is temperature (K); P is pressure (bar); m_{NaCl} is the molality of NaCl; AAD = $\Sigma|100(m_{cal}/m_{exp}-1)|/N_d$, where m_{cal} and m_{exp} are the calculated and experimental H_2S solubilities in aqueous NaCl solution, respectively, and N_d is the number of data points.

4.2. Water content of vapor phase in the H_2S–H_2O–NaCl system

At vapor-liquid equilibrium, the water content of vapor phase in the H_2S–H_2O–NaCl system can be calculated from the following relationship (Details see Appendix C):

$$y_{H_2O} = \frac{\varphi_{H_2O}^{H_2S-H_2O(V)} y_{H_2O}^{H_2S-H_2O(V)} x_{H_2O} \exp\left(-\frac{M_{H_2O}\phi}{1000}\sum(m_{Na^+}+m_{Cl^-})\right)}{\varphi_{H_2O}^{V} x_{H_2O}^{H_2S-H_2O(L)} x_{H_2O}^{NaCl-H_2O(L)}} \quad (16)$$

where y_{H_2O} and $\varphi_{H_2O}^{V}$ are the water content and fugacity coefficient of water in the vapor phase of the H_2S–H_2O–NaCl system, respectively. $x_{H_2O}^{H_2S-H_2O(L)}$ and $x_{H_2O}^{NaCl-H_2O(L)}$ are the mole fractions of water in the liquid phases of the H_2S–H_2O and NaCl–H_2O systems, respectively. $\varphi_{H_2O}^{H_2S-H_2O(V)}$ and $y_{H_2O}^{H_2S-H_2O(V)}$ are the fugacity coefficient and mole fraction of water in the vapor phase of the H_2S–H_2O system, respectively. x_{H_2O} is the mole fraction of water of liquid phase in the H_2S–H_2O–NaCl system, M_{H_2O} is the molar mass of H_2O, and ϕ is the osmotic coefficient of aqueous NaCl solution from Pitzer et al. (1984).

In Eq. (16), $\varphi_{H_2O}^{H_2S-H_2O(V)}$, $y_{H_2O}^{H_2S-H_2O(V)}$ and $x_{H_2O}^{H_2S-H_2O(L)}$ at given T and P can be calculated from the developed EOS of H_2S–H_2O mixture in Section 3, x_{H_2O} at given T, P and m_{NaCl} can be obtained from Eq. (15) in Section 4.1. Because the NaCl content in the vapor phase of the H_2S–H_2O–NaCl system is almost zero, y_{H_2O} can be calculated from Eq. (16) by a simple iterative approach assuming that the initial y_{H_2O} involved in $\varphi_{H_2O}^{V}$ equals to that of binary H_2S–H_2O system.

Table 9 lists the comparison of the water contents predicted by the model with the experimental data of Suleimenov and Krupp (1994). The deviations are all within experimental uncertainties up to 594 K and 138 bar. Fig. 5 compares the water content of vapor phase in the H_2S–H_2O–NaCl and CO_2–H_2O–NaCl mixtures as a function of pressure at given NaCl concentrations (2, 4 and 6 mol kg^{-1}) and temperatures (323.15 K, 393.15 K and 473.15 K). The water content of vapor phase in the CO_2–H_2O–NaCl mixture is estimated by combining the EOS of the CO_2–H_2O mixture from Gernert and Span (2016), the relative activity coefficient of CO_2 in aqueous NaCl solution from Mao et al. (2013) and the osmotic coefficient of aqueous NaCl solution from Pitzer et al. (1984). It can be seen from Fig. 5 that the predicted water

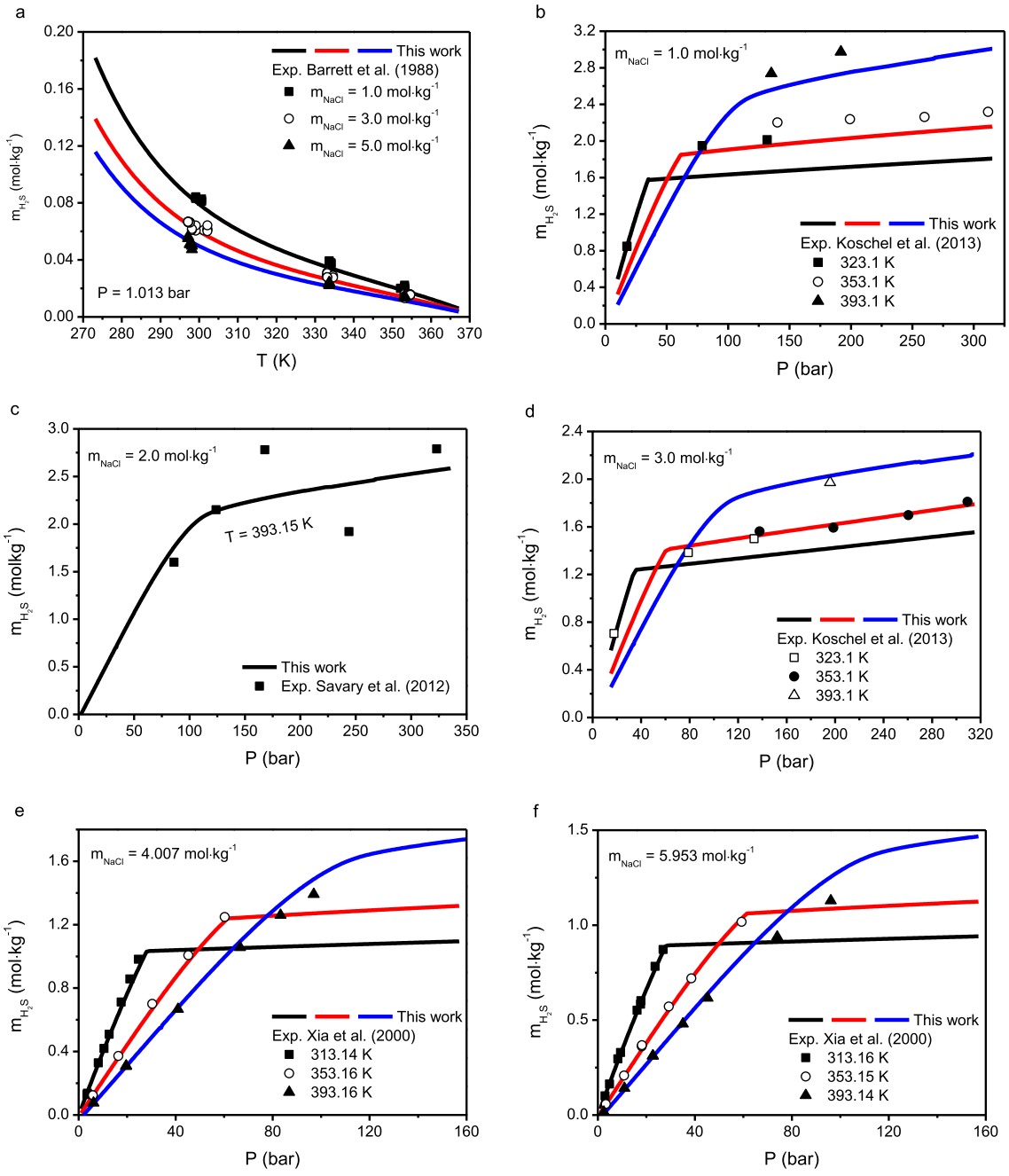

Fig. 3. Predicted H_2S solubility in aqueous NaCl solution: T is temperature, P is pressure. m_{H_2S} and m_{NaCl} are the molality of H_2S and NaCl, respectively.

content of vapor phase in the H_2S–H_2O–NaCl mixture is larger than that of the CO_2–H_2O–NaCl mixture under the same T-P-m_{NaCl} conditions, and their differences gradually reduce with the increase of temperatures.

4.3. The PVTx properties of the H_2S–H_2O–NaCl fluid mixture

In 2015, Mao et al. (2015b) proposed a predictive *PVTx* model for the CO_2–H_2O–NaCl fluid mixture by the Helmholtz free energy models of the binary CO_2–H_2O and H_2O–NaCl fluid mixtures. That model used no other mixing parameters but those of the CO_2–H_2O system, because the Helmholtz free energy of the H_2O–NaCl fluid at a given composition can be equivalently converted into that of pure H_2O by a scaled temperature redefined at the same pressure. Therefore, the predictive approach of Mao et al. (2015b) can also be used to calculate the *PVTx* properties of the H_2S–H_2O–NaCl mixture by combining the EOS of the H_2S–H_2O mixture developed here with the EOS of the H_2O–NaCl mixture from Mao et al. (2015b). Fig. 6 shows the calculated saturated liquid density of the H_2S–H_2O–NaCl mixture as a function of temperature at 200 bar and different salinities (0, 3 and 6 mol kg^{-1}), from which it can be seen that the saturated liquid density gradually decreases with the increase of temperature.

Up to now, no experimental volumetric data have been reported for the H_2S–H_2O–NaCl mixture, and future experimental studies are still needed to testify this predictive approach. However, the predictive *PVTx* model of Mao et al. (2015b) has been confirmed to be valid from 273 to 1273 K and from 0 to 5000 bar for the CO_2–H_2O–NaCl mixture of all fluid compositions, so this approach should be also valid for the H_2S–H_2O–NaCl fluid mixture.

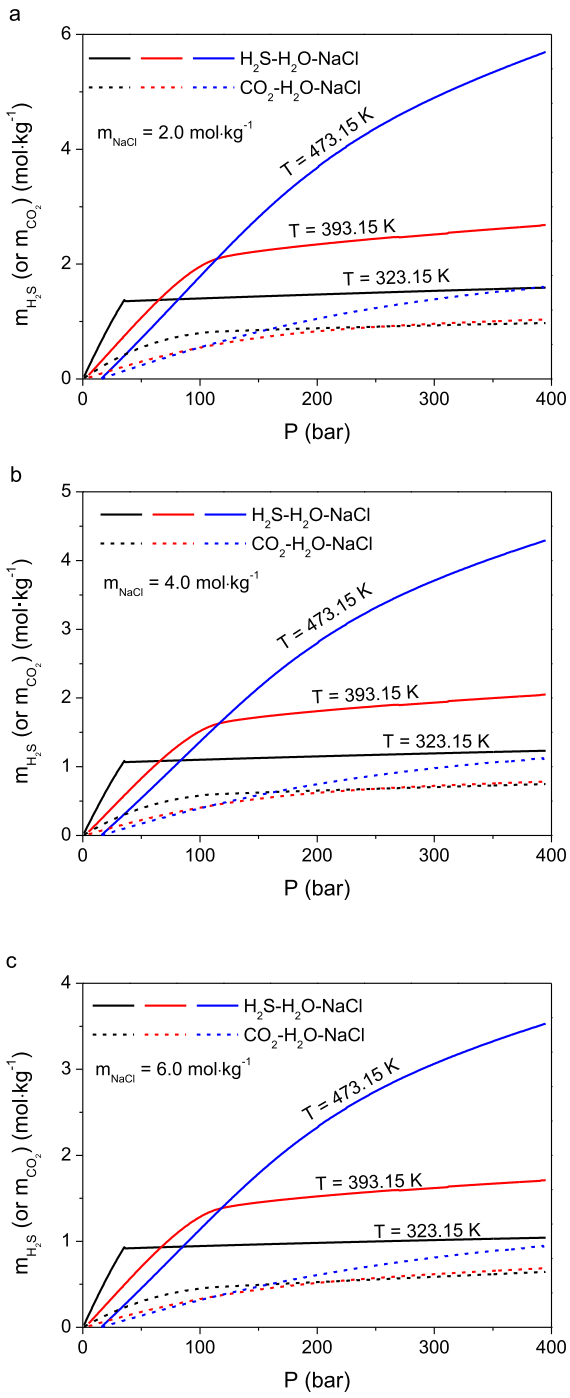

Fig. 4. Comparisons of the calculated H_2S and CO_2 solubilities in aqueous NaCl solution: T is temperature, P is pressure. m_{NaCl}, m_{H_2S} and m_{CO_2} are the molality of NaCl, H_2S and CO_2, respectively. Solid and short dash curves are for the H_2S–H_2O–NaCl and CO_2–H_2O–NaCl fluid mixtures, respectively.

5. Discussions

Table 2 lists the thermodynamic models for the VLE and *PVTx* properties of H_2S–H_2O and H_2S–H_2O–NaCl systems since 2000. It is unnecessary to compare our EOS with each model in Table 2. Here this developed EOS is compared with the other two typical models published recently: the models of Ji and Zhu (2012) and Akinfiev et al. (2016). We calculated the equilibrium compositions and saturated densities of the H_2S–H_2O mixture at temperatures up to 373.15 K and pressures up to 600 bar and compared them with the recommended values of Ji and Zhu (2012) (details see the excel file in the supplemental data). The differences in the saturated liquid densities of the H_2S–H_2O mixture between the two models are less than 1%. It should be noted that the liquid densities of the H_2S–H_2O mixture between this work and the experimental data of Hnědkovský et al. (1996) differ less than 0.1% at temperature up to 705.53 K and pressure up to 350 bar except for the data close to the critical pressure of pure H_2O. The differences of H_2S solubilities between this work and the model of Ji and Zhu (2012) except for the pressures below 10 bar are within 7%, which is within experimental uncertainty. The differences of water contents in the vapor phase of H_2S–H_2O system at low pressures are less than 8%. However, the calculated water contents in vapor phase between this work and Ji and Zhu (2012) exhibit large differences when pressure is above the critical pressure of pure H_2S. However, the prediction of this work is much closer to the experimental data as shown in Fig. 2. For example, at 373 K and 20 bar the experimental water content in vapor phase is 0.0081, and the values of this work and Ji and Zhu (2012) are 0.0080 and 0.0071, respectively.

Table 9
Comparison of the predicted water content with the experimental data of H_2S–H_2O–NaCl system from Suleimenov and Krupp (1994).

T (K)	P (bar)	m_{NaCl} (mol·kg^{-1})	$y_{H_2O,exp}$	$y_{H_2O,cal}$	Dev (%)
428.45	11.96	0.501397	0.462270	0.465269	0.65
428.35	12.14	0.917460	0.448099	0.451238	0.70
428.45	12.37	1.266488	0.435890	0.439055	0.73
428.55	12.65	1.565157	0.423268	0.426341	0.73
428.55	12.92	1.813737	0.411168	0.414087	0.71
428.55	13.12	2.031992	0.401964	0.404765	0.70
428.45	13.42	2.224016	0.389725	0.392295	0.66
428.45	13.71	2.391065	0.379585	0.381958	0.63
428.35	14.05	2.539914	0.367981	0.370107	0.58
489.65	27.6	0.235305	0.791553	0.801313	1.23
489.65	27.58	0.633844	0.781067	0.792059	1.41
489.55	27.46	0.963825	0.773444	0.785569	1.57
489.45	27.43	1.244519	0.764886	0.777906	1.70
489.45	27.48	1.485776	0.756787	0.770525	1.82
489.55	27.56	1.693200	0.750234	0.764579	1.91
489.45	27.7	1.878675	0.740285	0.754995	1.99
489.45	27.87	2.043342	0.731613	0.746620	2.05
593.95	137.86	0.488358	0.887485	0.874649	−1.45
593.65	137.38	0.888102	0.873170	0.866247	−0.79
593.75	137.21	1.224310	0.862612	0.861099	−0.18
593.65	137.54	1.515965	0.850452	0.853244	0.33
593.55	137.9	1.765112	0.839670	0.846083	0.76
593.55	138.42	1.981011	0.830236	0.839725	1.14

Notes: T is temperature; P is pressure; $y_{H_2O,exp}$ and $y_{H_2O,cal}$ are the experimental and calculated water content (in mole fraction) of vapor phase of the H_2S–H_2O–NaCl system, respectively; Dev = $100(y_{H_2O,cal}/y_{H_2O,exp}-1)$.

The H_2S solubilities calculated from this work are also compared with those from the Akinfiev et al. (2016) model at temperatures up to 573.15 K, pressures up to 600 bar and NaCl concentrations up to 6 mol kg^{-1}. The differences in solubilities at temperatures below 473.15 K are close to the experimental uncertainty, but the solubilities of this work differ those of Akinfiev et al. (2016) by more than 20% at pressures above 300 bar when the temperatures are 523.15 K and 573.15 K. One reason might be that the parameters in this work are constrained by both the water-rich and H_2S-rich phases, which is unlike the approach of Akinfiev et al. (2016). Another reason is that there is no high-pressure phase equilibrium data for the H_2S–H_2O and H_2S–H_2O–NaCl mixtures at high temperatures. Therefore, the recommended *T-P-*m_{NaCl} range is 273–473 K, 0–400 bar and 0–6 mol kg^{-1} in this work.

The strength of this work is that the established thermodynamic models can satisfactorily reproduce the VLE and *PVTx* data of the H_2S–H_2O and H_2S–H_2O–NaCl mixtures, and have certain extrapolated ability. This work can be used to estimate the content of the dissolved H_2S gas in formation water and the density of solution during the

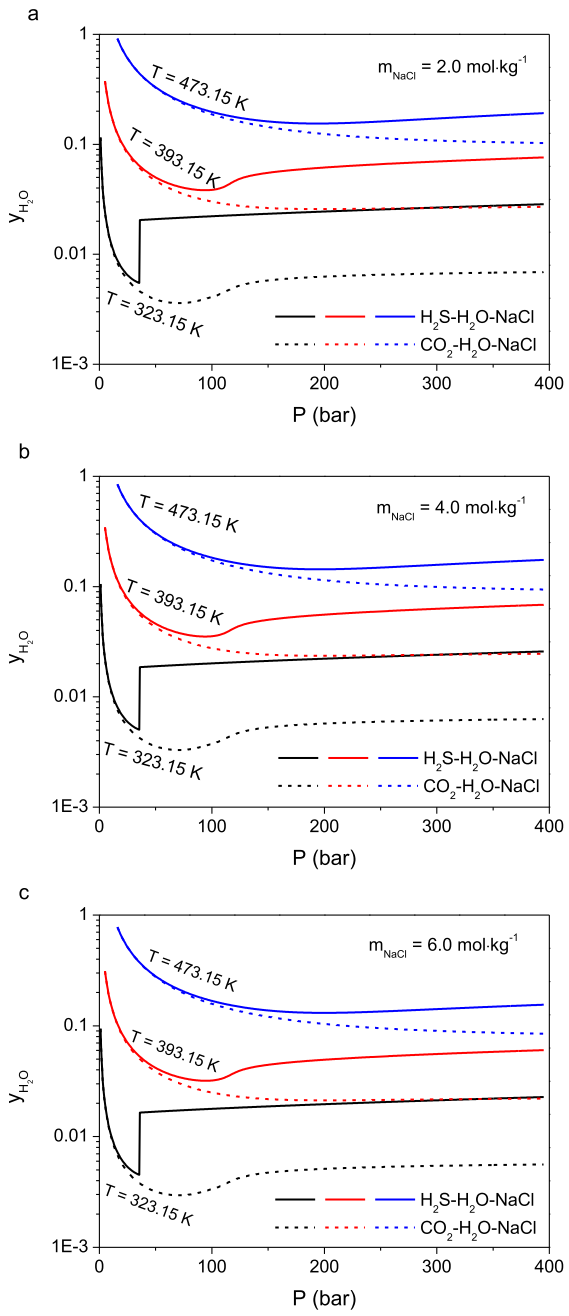

Fig. 5. Predicted water content of vapor phase for the ternary H_2S-H_2O−NaCl and CO_2−H_2O−NaCl fluid mixtures: T is temperature, P is pressure, m_{NaCl} is the molality of NaCl, and y_{H_2O} is the mole fraction of H_2O. Solid and short dash curves are for the H_2S−H_2O−NaCl and CO_2−H_2O−NaCl fluid mixtures, respectively.

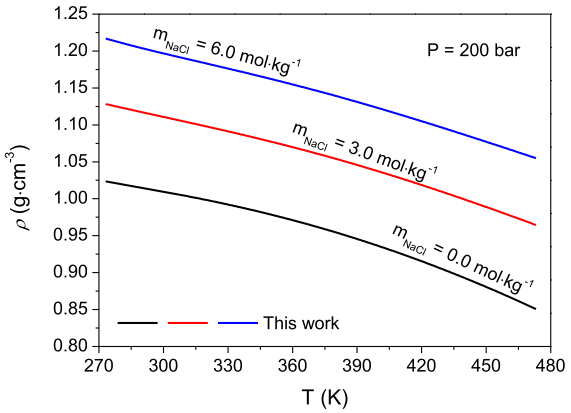

Fig. 6. Calculated saturated liquid density of the H_2S-H_2O−NaCl fluid mixture: T is temperature, P is pressure, m_{NaCl} is the molality of NaCl, and ρ is the liquid density with saturated H_2S.

exploit process of H_2S-bearing natural gas well or when CO_2 and H_2S is sequestrated in deep saline formations. Owning to the complexity of the developed models and different iterative methods used in the calculation, the computer codes are provided in Appendix D (supplementary data) for easy application.

6. Conclusions

A dimensionless Helmholtz free energy EOS for the H_2S−H_2O fluid mixture has been developed by using five mixing parameters, from which the VLE and *PVTx* properties can be calculated by thermodynamic relations. The developed EOS can accurately reproduce the VLE properties of the H_2S−H_2O fluid mixtures up to 473 K and 400 bar within or close to experimental uncertainties. Compared to other empirical approaches that exist in literature, this work can satisfactorily predict both the equilibrium compositions of vapor and liquid phase and the volumetric properties for the H_2S−H_2O mixture covering a wide temperature-pressure range.

The EOS of the H_2S−H_2O mixture, combined with the Pitzer activity coefficient of H_2S in aqueous NaCl solution, the osmotic coefficient of aqueous NaCl solution and the EOS of the H_2O−NaCl mixture, is extended to predict the VLE and *PVTx* properties of the H_2S−H_2O−NaCl mixture under the conditions of CCS (T-P-m_{NaCl} range of 273–473 K, 0–400 bar and 0–6 mol kg^{-1}). It should be noted that experimental volumetric data are still lacking for the H_2S−H_2O and H_2S−H_2O−NaCl mixtures, and experimental studies can be focused on the volumetric properties of these systems in the future.

Acknowledgements

This work is jointly supported by the National Natural Science Foundation of China (Grant No. 41673065) and the National Key Basic Research Development Program (Grant No. 2015CB452606).

Appendix A. The Helmholtz free energy model of H_2S fluid

The VLE and *PVT* properties of pure H_2S are calculated from the Helmholtz free energy model of Li (2017), where $\alpha^r_{H_2S}$, the residual part of dimensionless Helmholtz free energy of H_2S, takes the form of Sun and Ely (2004).

$$\alpha^r_{H_2S} = \sum_{m=1}^{6} a_m \tau^{j_m} \delta^{i_m} + \sum_{m=7}^{14} a_m \tau^{j_m} \delta^{i_m} e^{-\delta^{k_m}} \quad (A1)$$

$$\tau = \frac{T_{c,i}}{T}, \quad \delta = \frac{\rho}{\rho_{c,i}} \quad (A2)$$

where T is the temperature in K, ρ is the density of H_2S, $T_{c,i}$ and $\rho_{c,i}$ are the critical temperature and pressure of H_2S, respectively, and δ and τ are the reduced parameters. The coefficients a_m and the exponents i_m, j_m and k_m are listed in Table A1.

Table A1
Values for the parameters of Eq. (A1) (Taken from Li (2017)).

m	a_m	i_m	j_m	k_m
1	0.67919879	1	1.5	0
2	0.85733637	1	0.25	0
3	$-0.25565454 \times 10^{1}$	1	1.25	0
4	$0.59741335 \times 10^{-1}$	3	0.25	0
5	$0.19438086 \times 10^{-3}$	7	0.875	0
6	$-0.67511619 \times 10^{-2}$	2	1.375	0
7	$0.42367115 \times 10^{-1}$	1	0	1
8	$0.52412880 \times 10^{-1}$	1	2.375	1
9	0.22234326	2	2	1
10	$-0.42165405 \times 10^{-2}$	5	2.125	1
11	−0.22313308	1	3.5	2
12	$-0.72782985 \times 10^{-3}$	1	6.5	2
13	$-0.32108703 \times 10^{-1}$	4	4.75	2
14	$-0.88550287 \times 10^{-2}$	2	12.5	3

Appendix B. The Pitzer parameters of Duan et al. (2007).

The Pitzer parameters of Duan et al. (2007) related to Eq. (14) are listed in Table B1.

Table B1
Coefficients of Eqs. (14)–(16).

	$\lambda_{H_2S\text{-}Na^+}$	$\xi_{H_2S\text{-}Cl^-\text{-}Na^+}$
c_1	8.5004999×10^{-2}	
c_2	3.5330378×10^{-5}	
c_3	−1.5882605	
c_4	1.1894926×10^{-5}	
c_5		$-1.0832589 \times 10^{-2}$

Appendix C. The water content of vapor phase in the H_2S–H_2O–NaCl system

At vapor-liquid equilibrium, the water content of vapor phase in the H_2S–H_2O–NaCl system can be calculated from the following fugacity-activity relation:

$$y_{H_2O} = f^{*(L)}_{H_2O}\gamma^{L}_{H_2O}x_{H_2O}/\left(\varphi^{V}_{H_2O}P\right) \tag{C1}$$

where y_{H_2O} is the water content of vapor phase in the H_2S–H_2O–NaCl system, $f^{*(L)}_{H_2O}$ is the fugacity of pure water in liquid phase, $\gamma^{L}_{H_2O}$ is the activity coefficient of water in liquid phase, x_{H_2O} is the mole fraction of water in liquid phase, and $\varphi^{V}_{H_2O}$ is the fugacity coefficient of water in vapor phase.

The $\gamma^{L}_{H_2O}$ in Eq. (C1) can be approximated by

$$\gamma^{L}_{H_2O} = \gamma^{H_2S-H_2O(L)}_{H_2O}\gamma^{NaCl-H_2O(L)}_{H_2O} \tag{C2}$$

where $\gamma^{H_2S-H_2O(L)}_{H_2O}$ is the activity coefficient of water in the liquid phase of binary H_2S–H_2O system, and $\gamma^{NaCl-H_2O(L)}_{H_2O}$ is the activity coefficient of water in the liquid phase of binary NaCl–H_2O system.

The $\gamma^{H_2S-H_2O(L)}_{H_2O}$ can be obtained by

$$\gamma^{H_2S-H_2O(L)}_{H_2O} = y^{H_2S-H_2O(V)}_{H_2O}\varphi^{H_2S-H_2O(V)}_{H_2O}P/\left(f^{*(L)}_{H_2O}x^{H_2S-H_2O(L)}_{H_2O}\right) \tag{C3}$$

where $\varphi^{H_2S-H_2O(V)}_{H_2O}$ is the fugacity coefficient of water in the vapor phase of the H_2S–H_2O system, and $y^{H_2S-H_2O(V)}_{H_2O}$ and $x^{H_2S-H_2O(L)}_{H_2O}$ are the mole fractions of water in the vapor and liquid phases of the H_2S–H_2O system, respectively.

The $\gamma^{NaCl-H_2O(L)}_{H_2O}$ in Eq. (C2) can be obtained by

$$\gamma^{NaCl-H_2O(L)}_{H_2O} = a^{NaCl-H_2O(L)}_{H_2O}/x^{NaCl-H_2O(L)}_{H_2O} \tag{C4}$$

where $a^{NaCl-H_2O(L)}_{H_2O}$ and $x^{NaCl-H_2O(L)}_{H_2O}$ are the activity and the mole fraction of water in the liquid phase of the NaCl–H_2O system, respectively. $a^{NaCl-H_2O(L)}_{H_2O}$ here is calculated from the highly accurate equation of Pitzer et al. (1984):

$$a^{NaCl-H_2O}_{H_2O} = \exp\left(-\frac{M_{H_2O}\phi}{1000}\sum\left(m_{Na^+} + m_{Cl^-}\right)\right) \tag{C5}$$

where M_{H_2O} is the molar mass of H_2O, and ϕ is the osmotic coefficient of aqueous NaCl solution (Pitzer et al., 1984).

Substituting Eq. (C2) to (C5) into Eq. (C1) yields the final equation:

$$y_{H_2O} = \frac{\varphi_{H_2O}^{H_2S-H_2O(V)} y_{H_2O}^{H_2S-H_2O(V)} x_{H_2O} \exp\left(-\frac{M_{H_2O}\phi}{1000}\sum (m_{Na^+} + m_{Cl^-})\right)}{\varphi_{H_2O}^{V} x_{H_2O}^{H_2S-H_2O(L)} x_{H_2O}^{NaCl-H_2O(L)}} \quad (C6)$$

Appendix D. Supplemental data

For easy application, a compressed file is provided, where four f90 files programed in Fortran language can calculate the VLE and *PVTx* properties of H_2S-H_2O and $H_2S-H_2O-NaCl$ fluid mixtures, and one excel file shows the comparisons between our model and experimental data and the models of Ji and Zhu (2012) and Akinfiev et al. (2016).

Appendix E. Supplementary data

Supplementary data to this article can be found online at https://doi.org/10.1016/j.apgeochem.2018.12.021.

References

Akinfiev, N.N., Majer, V., Shvarov, Y.V., 2016. Thermodynamic description of H_2S-H_2O-NaCl solutions at temperatures to 573 K and pressures to 40 MPa. Chem. Geol. 424, 1–11.

Bacon, D.H., Ramanathan, R., Schaef, H.T., McGrail, B.P., 2014. Simulating geologic co-sequestration of carbon dioxide and hydrogen sulfide in a basalt formation. International Journal of Greenhouse Gas Control 21, 165–176.

Barrett, T.J., Anderson, G.M., Lugowski, J., 1988. The solubility of hydrogen sulfide in 0 − 5 M NaCl solutions at 25 °C − 95 °C and one atmosphere. Geochem. Cosmochim. Acta 52, 807–811.

Burgess, M.P., Germann, R.P., 1969. Physical properties of hydrogen sulfide-water mixtures. AIChE J. 15, 272–275.

Byeseda, J.J., Deetz, J.A., Manning, W.P., 1985. The OPTISOL gas sweetening solvent. In: Laurance Reid Gas Conditioning Conference Norman Oklahoma, pp. C1–C15.

Cai, C., Hu, G., Li, H., Jiang, L., He, W., Zhang, B., Jia, L., Wang, T., 2015. Origins and fates of H_2S in the Cambrian and Ordovician in Tazhong area: evidence from sulfur isotopes, fluid inclusions and production data. Mar. Petrol. Geol. 67, 408–418.

Chapoy, A., Mohammadi, A.H., Tohidi, B., Valtz, A., Richon, D., 2005. Experimental measurement and phase behavior modeling of hydrogen sulfide-water binary system. Ind. Eng. Chem. Res. 44, 7567–7574.

Clarke, E.C.W., Glew, D.N., 1971. Aqueous nonelectrolyte solutions. Part VIII. Deuterium and hydrogen sulfides solubilities in deuterium oxide and water. Can. J. Chem. 49, 691–698.

Dede, L., Becker, T., 1926. The manipulation of sulfide precipitation through the addition of neutral salts. Zeitschrift fur Anorganische und Allgemeine Chemie 152, 185–196.

dos Ramos, M.C., McCabe, C., 2010. Modeling the phase behavior, excess enthalpies and Henry's constants of the H_2O + H_2S binary mixture using the SAFT-VR + D approach. Fluid Phase Equil. 290, 137–147.

Douabul, A.A., Riley, J.P., 1979. The solubility of gases in distilled water and seawater–V. hydrogen sulphide. Deep Sea Res. Oceanogr. Res. Pap. 26A, 259–268.

Drummond, S.E., 1981. Boiling and Mixing of Hydrothermal Fluids: Chemical Effects on Mineral Precipitation. Ph. D. Dissertation. Geosciences. Pennsylvania State University, pp. 380.

Duan, Z., Sun, R., Liu, R., Zhu, C., 2007. Accurate thermodynamic model for the calculation of H_2S solubility in pure water and brines. Energy Fuels 21, 2056–2065.

Dubessy, J., Tarantola, A., Sterpenich, J., 2005. Modelling of liquid-vapour equilibria in the H_2O-CO_2-NaCl and H_2O-H_2S-NaCl systems to 270 °C. Oil Gas Sci. Technol. 60, 339–355.

Emami-Meybodi, H., Hassanzadeh, H., Green, C.P., Ennis-King, J., 2015. Convective dissolution of CO_2 in saline aquifers: progress in modeling and experiments. International Journal of Greenhouse Gas Control 40, 238–266.

Firoozabadi, A., Myint, P.C., 2010. Prospects for subsurface CO_2 sequestration. AIChE J. 56, 1398–1405.

Gernert, J., Span, R., 2016. EOS–CG: a Helmholtz energy mixture model for humid gases and CCS mixtures. J. Chem. Therm. 93, 274–293.

Gerrard, W., 1972. Solubility of hydrogen sulphide, dimethyl ether, methyl chloride and sulphur dioxide in liquids. The prediction of solubility of all gases. Journal of Applied Chemistry & Biotechnology 22, 623–650.

Gillespie, P.C., Wilson, G.M., 1982. Vapour-liquid and Liquid-liquid Equilibria: Water-methane, Water-carbon Dioxide, Water-hydrogen Sulphide, Water-pentane. Gas Processors Association Research Report RR-48 Project 758-B-77.

Giuliani, G., Dubessy, J., Banks, D., Vinh, H.Q., Lhomme, T., Pironon, J., Garnier, V., Trinh, P.T., Van Long, P., Ohnenstetter, D., Schwarz, D., 2003. CO_2-H_2S-COS-S_8-AlO(OH)-bearing fluid inclusions in ruby from marble-hosted deposits in Luc Yen area, North Vietnam. Chem. Geol. 194, 167–185.

Gunter, W.D., Perkins, E.H., Hutcheon, I., 2000. Aquifer disposal of acid gases: modelling of water-rock reactions for trapping of acid wastes. Appl. Geochem. 15, 1085–1095.

Harkness, A.C., Kelman, B.A., 1967. Solubility of methyl mercaptan in water. TAPPI (Tech. Assoc. Pulp Pap. Ind.) 50, 13.

Hnědkovský, L., Wood, R.H., Majer, V., 1996. Volumes of aqueous solutions of CH_4, CO_2, H_2S, and NH_3 at temperatures from 298.15 K to 705 K and pressures to 35 MPa. J. Chem. Therm. 28, 125–142.

Jafari Raad, S.M., Hassanzadeh, H., 2017. Prospect for storage of impure carbon dioxide streams in deep saline aquifers—a convective dissolution perspective. International Journal of Greenhouse Gas Control 63, 350–355.

Ji, X.Y., Zhu, C., 2010. Modeling of phase equilibria in the H_2S-H_2O system with the statistical associating fluid theory. Energy Fuels 24, 6208–6213.

Ji, X.Y., Zhu, C., 2012. A SAFT equation of state for the quaternary H_2S-CO_2-H_2O-NaCl system. Geochem. Cosmochim. Acta 91, 40–59.

Kapustinsky, A.A.,R.I., 1941. Setschenoff's rule and the solubility of hydrogen sulphide in hydrochloric acid solutions. Comptes Rendus del Academie des Sciences del Urss 30, 625–628.

Kendall, J., Andrews, J.C., 1921. The solubilities of acids in aqueous solutions of other acids. J. Am. Chem. Soc. 43, 1545–1560.

Kiss, Á.v., Lajtai, I., Thury, G., 1937. Über die löslichkeit von gasen in wasser-Nichtelektrolytgemischen. Z. Anorg. Chem. 233, 346–352.

Knauss, K.G., Johnson, J.W., Steefel, C.I., 2005. Evaluation of the impact of CO_2, co-contaminant gas, aqueous fluid and reservoir rock interactions on the geologic sequestration of CO_2. Chem. Geol. 217, 339–350.

Koschel, D., Coxam, J.-Y., Majer, V., 2007. Enthalpy and solubility data of H_2S in water at conditions of interest for geological sequestration. Ind. Eng. Chem. Res. 46, 1421–1430.

Koschel, D., Coxam, J.-Y., Majer, V., 2013. Enthalpy and solubility data of H_2S in aqueous salt solutions at conditions of interest for geological sequestration. Ind. Eng. Chem. Res. 52, 14483–14491.

Kozintseva, T.N., 1965. Rostvorimost serovodoroda v vode i solevykh rastvorakh pri povyshenykh temperaturakh. Geokhimicheskie issledovaniya v oblasti povyshennykh davlenii i temperatur 121–134.

Kunz, O., Wagner, W., 2012. The GERG-2008 wide-range equation of state for natural gases and other mixtures: an expansion of GERG-2004. J. Chem. Eng. Data 57, 3032–3091.

Kuranov, G., Rumpf, B., Smirnova, N.A., Maurer, G., 1996. Solubility of single gases carbon dioxide and hydrogen sulfide in aqueous solutions of N-Methyldiethanolamine in the temperature range 313 − 413 K at pressures up to 5 MPa. Ind. Eng. Chem. Res. 35, 1959–1966.

Lee, J.I., Mather, A.E., 1977. Solubility of hydrogen sulfide in water. Ber. Bunsen Ges. Phys. Chem. 81, 1020–1023.

Li, J., Wei, L., Li, X., 2015. An improved cubic model for the mutual solubilities of CO_2-CH_4-H_2S-brine systems to high temperature, pressure and salinity. Appl. Geochem. 54, 1–12.

Li, J., Xie, Z.Y., Dai, J.X., Zhang, S.C., Zhu, G.Y., Liu, Z.L., 2005. Geochemistry and origin of sour gas accumulations in the northeastern Sichuan Basin, SW China. Org. Geochem. 36, 1703–1716.

Li, X., 2017. The prediction of *PVTx* and VLE properties of C-H-O-N-S fluid mixtures (Dissertation). In: Earth Sciences and Resources. China University of Geosciences, pp. 101.

Li, Z., Firoozabadi, A., 2009. Cubic-plus-association equation of state for water-containing mixtures: is "cross association" necessary? AIChE J. 55, 1803–1813.

Mao, S., Deng, J., Lü, M., 2015a. A Helmholtz free energy equation of state for the NH_3-H_2O fluid mixture: correlation of the *PVTx* and vapor–liquid phase equilibrium properties. Fluid Phase Equil. 393, 26–32.

Mao, S., Hu, J., Zhang, Y., Lü, M., 2015b. A predictive model for the *PVTx* properties of CO_2-H_2O-NaCl fluid mixture up to high temperature and high pressure. Appl. Geochem. 54, 54–64.

Mao, S., Zhang, D., Li, Y., Liu, N., 2013. An improved model for calculating CO_2 solubility in aqueous NaCl solutions and the application to CO_2-H_2O-NaCl fluid inclusions. Chem. Geol. 347, 43–58.

McLauchlan, W., 1903. On the influence of salts on the water-solubility of sulphuric hydrogen, iodine and bromine. Zeitschrift fur Physikalische Cheme-Stochiometrie und Verwandtschaftslehre 44, 600–633.

Michelsen, M.L., 1993. Phase equilibrium calculations. What is easy and what is difficult? Comput. Chem. Eng. 17, 431–439.

Perfetti, E., Thiery, R., Dubessy, J., 2008. Equation of state taking into account dipolar interactions and association by hydrogen bonding: II - modelling liquid-vapour equilibria in the H_2O-H_2S, H_2O-CH_4 and H_2O-CO_2 systems. Chem. Geol. 251, 50–57.

Pitzer, K.S., Peiper, J.C., Busey, R.H., 1984. Thermodynamic properties of aqueous sodium-chloride solutions. J. Phys. Chem. Ref. Data 13, 1–102.

Pohl, H.A., 1961. Thermodynamics of the hydrogen sulfide-water-system relevant to the

dual temperature process for the production of heavy water. J. Chem. Eng. Data 6, 515–521.
Pollitzer, F., 1909. Über das gleichgewicht der reaktion H_2S + 2J = 2HJ + S und die dissoziation des schwefelwasserstoffs. Z. Anorg. Chem. 64, 121–148.
Savary, V., Berger, G., Dubois, M., Lacharpagne, J.-C., Pages, A., Thibeau, S., Lescanne, M., 2012. The solubility of CO_2 + H_2S mixtures in water and 2 M NaCl at 120 °C and pressures up to 35 MPa. International Journal of Greenhouse Gas Control 10, 123–133.
Selleck, F.T., Carmichael, L.T., Sage, B.H., 1952. Phase behavior in the hydrogen sulfide-water system. Ind. Eng. Chem. 44, 2219–2226.
Soreide, I., Whitson, C.H., 1992. Peng-Robinson predictions for hydrocabons, CO_2, N_2, and H_2S with pure water and NaCl brine. Fluid Phase Equil. 77, 217–240.
Springer, R.D., Wang, P.M., Anderko, A., 2015. Modeling the properties of H_2S/CO_2/salt/water systems in wide ranges of temperature and pressure. SPE J. 20, 1120–1134.
Suleimenov, O.M., Krupp, R.E., 1994. Solubility of hydrogen sulfide in pure water and in NaCl solutions, from 20 to 320 °C and at saturation pressures. Geochem. Cosmochim. Acta 58, 2433–2444.
Sun, L., Ely, J.F., 2004. Universal equation of state for engineering application: algorithm and application to non-polar and polar fluids. Fluid Phase Equil. 222–223, 107–118.
Tsivintzelis, I., Kontogeorgis, G.M., Michelsen, M.L., Stenby, E.H., 2010. Modeling phase equilibria for acid gas mixtures using the CPA equation of state. I. Mixtures with H_2S. AIChE J. 56, 2965–2982.
Wagner, W., Pruss, A., 2002. The IAPWS formulation 1995 for the thermodynamic properties of ordinary water substance for general and scientific use. J. Phys. Chem. Ref. Data 31, 387–535.
Winkler, L.W., 1906. Regularity of absorption of gases in liquids. Zeitschrift fur Physikalische Chemie 55, 344–354.
Worden, R.H., Smalley, P.C., Oxtoby, N.H., 1995. Gas souring by thermochemical sulfate reduction at 140 degrees C. Aapg Bulletin-American Association of Petroleum Geologists 79, 854–863.
Wright, R.H., Maass, O., 1932a. Electrical conductivity of aqueous solutions of hydrogen sulphide and the state of the dissolved gas. Can. J. Res. 6, 588–595.
Wright, R.H., Maass, O., 1932b. Solubility of hydrogen sulphide in water from the vapour pressures of the solutions. Can. J. Res. 6, 94–101.
Xia, J., Pérez-Salado Kamps, Á., Rumpf, B., Maurer, G., 2000. Solubility of hydrogen sulfide in aqueous solutions of the single salts sodium sulfate, ammonium sulfate, sodium chloride, and ammonium chloride at temperatures from 313 to 393 K and total pressures up to 10 MPa. Ind. Eng. Chem. Res. 39, 1064–1073.
Zezin, D.Y., Migdisov, A.A., Williams-Jones, A.E., 2011. *PVTx* properties of H_2O-H_2S fluid mixtures at elevated temperature and pressure based on new experimental data. Geochem. Cosmochim. Acta 75, 5483–5495.
Zirrahi, M., Azin, R., Hassanzadeh, H., Moshfeghian, M., 2012. Mutual solubility of CH_4, CO_2, H_2S, and their mixtures in brine under subsurface disposal conditions. Fluid Phase Equil. 324, 80–93.